

EmoHead: Emotional Talking Head via Manipulating Semantic Expression Parameters

Xuli Shen^{1,2} Hua Cai² Dingding Yu² Weilin Shen² Qing Xu² Xiangyang Xue^{1*}

¹Fudan University

²UniDT

<https://bisno.github.io/Emohead>

Abstract—Generating emotion-specific talking head videos from audio input is an important and complex challenge for human-machine interaction. However, emotion is highly abstract concept with ambiguous boundaries, and it necessitates disentangled expression parameters to generate emotionally expressive talking head videos. In this work, we present EmoHead to synthesize talking head videos via semantic expression parameters. To predict expression parameter for arbitrary audio input, we apply an audio-expression module that can be specified by an emotion tag. This module aims to enhance correlation from audio input across various emotions. Furthermore, we leverage pre-trained hyperplane to refine facial movements by probing along the vertical direction. Finally, the refined expression parameters regularize neural radiance fields and facilitate the emotion-consistent generation of talking head videos. Experimental results demonstrate that semantic expression parameters lead to better reconstruction quality and controllability.

Index Terms—emotional talking head synthesis, video manipulation, multi-modality alignment

I. INTRODUCTION

Talking head synthesis is the process of reanimating a target person to align with lip movement and head poses executed by input audio [1]–[5]. It involves the seamless integration of the audio source and target avatar, resulting in a realistic and synchronized video output by harnessing modern generative reconstruction methods [6], [7].

Emotional talking head synthesis, on the other hand, aims to generate talking avatar videos with vivid expressions for specific emotions [8]–[10]. Benefiting from the facial morphable model [11], [12], there are end-to-end methods that focus on audio-driven [9] or video-driven [10] pipelines that empower with facial expression editing capabilities. [13].

Nevertheless, these expression parameters are often entangled, which leads to the “**expression collapse**” phenomenon in reconstructed results, as depicted by the angry eye region for the target happy emotion in Fig. 1. We hypothesize that if the expression parameters are sufficiently refined, this phenomenon will be eliminated and emotional consistency will be improved, as seen in the smiling eye region of Fig. 1. In this work, we propose an target emotion expression refinement method to enhance the overall authenticity and effectiveness of emotional talking head synthesis. By accurately representing and refining facial movements, the framework enables more engaging and emotionally resonant experiences.

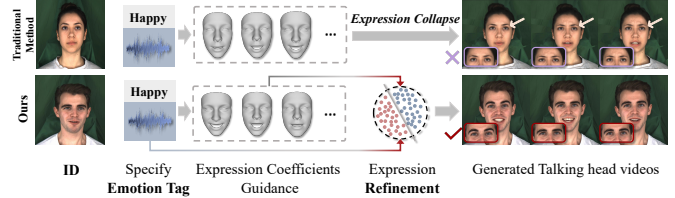


Fig. 1: Different from previous work, the proposed method applies emotion-specific hyperplanes to eliminate “expression collapse” phenomenon and generate target emotional videos.

Specifically, we present an audio-expression module that regresses low-dimensional expression parameters based on audio input from various sources and specific emotion categories. To better synchronize emotional talking videos, we first obtain the embedded audio feature and use timestamp-aligned audio speech recognition alongside pretrained audio-emotion encoder and text encoder to extract emotion features in audio and text features, respectively. We then propose an emotional cross-modality fusion mechanism, named Audio Expression Alignment, to eliminate noise emotions and preserve strong correlations. Next, we train emotion-specific hyperplanes to intricately refine and control facial movements through the low-dimensional expression parameters. Next, we leverage the predicted expression parameters and construct emotion-conditional implicit function for talking head reconstruction using volume rendering, and achieve high-fidelity synthesis with better controllability. Our key contributions are:

- We present an audio-expression module for mapping audio features to low-dimensional expression parameters. We propose Audio Expression Alignment, a cross-modality attention mechanism that enhances the correlation between audio features and emotion target.
- We apply an expression refinement method to enhance the emotion consistency of expression parameters and manipulate emotion representation in the talking stage.
- We leverage refined facial expression parameters for portrait rendering, resulting in better reconstruction quality and controllability of the target emotion.

II. RELATED WORK

A. Audio-Driven Talking Head Generation

Existing audio-driven talking head generation can be divided into identification-specific [2]–[5] and identification-

*Corresponding author.

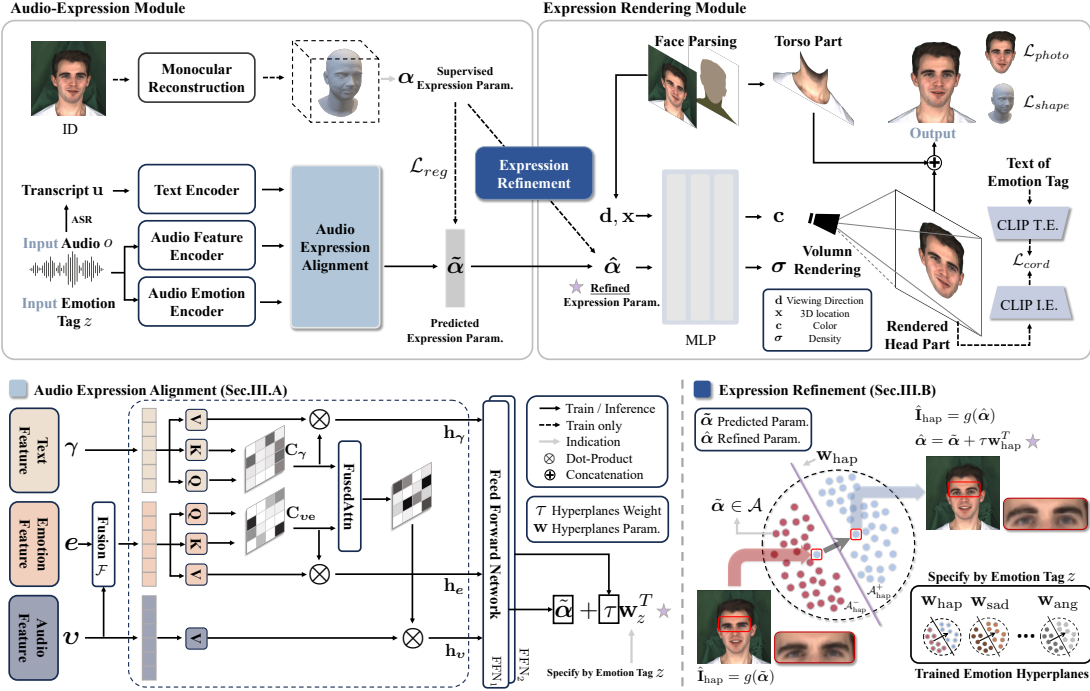


Fig. 2: The proposed framework of EmoHead.

agnostic [14], [15] fields. Identification-specific audio-driven talking head generation aims to synthesize videos of specifically trained target individuals. Recently, Style2Talker [5] learns personalized speaker-specific diffusion models using 3DMM coefficients and then generates videos via CLIP [16] guidance. In the field of identification-agnostic methods, talking head videos are generated in a one-shot setting, building a universal model applicable across different individuals. Specifically, SadTalker [17] learns decoupled and realistic motion coefficients from audio inputs. LivePortrait [15] drives arbitrary talking faces with audio while allowing free pose control by learning pose motions from another video source.

B. Emotional Talking Head Generation

Emotional talking head generation requires both emotional manipulation and high-fidelity generation method. In recent years, [8], [9], [18], [19] has focused on generating one-shot talking head animations with emotion control by providing an identity source image and an emotion source video. EAMM [19] leverages emotion discriminative loss for emotion talking head videos. EDTalk [20] aims to decompose the facial dynamics to enhance emotion representation. EAT [10] focuses on controlling the emotion via prompt. Nevertheless, few efforts have attempted to explore precise emotion representation for emotional talking head synthesis in cases where different emotions couple together.

III. METHOD

In this section, we present emotional talking head synthesis framework EmoHead, illustrated in Fig. 2. First, we

demonstrate the audio-expression module, which predicts facial expression parameters from multi-modality features. Next, we introduce a novel expression parameters refinement via trained hyperplane that classifies the target emotion. Then, we elaborate on the expression rendering module, which uses the expression parameters to synthesize 2D talking head videos via neural radiance field. Finally, we discuss key training details. **Task Formulation.** We aim to synthesize talking face video given specific emotion tag. The input audio state s is a pair (o, z) where o is a fixed-length audio and z is the tag of required emotion state. The goal of the task is to learn a function $\mathcal{G} : s \rightarrow \alpha \rightarrow \mathcal{I}$, where \mathcal{I} is the set of output frames and $\alpha \in \mathbb{R}^m$ refers to expression parameter.

A. Audio-Expression Module

Given the audio input frame i , we obtain the audio features \tilde{v}_i , and emotional features $\tilde{\mathbf{e}}_i$ present in the audio o_i using HuBERT-base as audio feature encoder [21] and Emotion2vec-base [22] as audio emotion encoder. Next, we utilize audio speech recognition (ASR [23]) to provide transcript \mathbf{u} , which is timestamp-aligned by audio (see Appendix.C). Then, we leverage the large language model LLaMa2-7b [24] to encode text features $\tilde{\gamma}_i$. We apply three different trainable linear mappings \mathbf{E} to project all the above features into same dimension d :

$$\mathbf{v}_i = \tilde{v}_i \mathbf{E}_1; \quad \mathbf{e}_i = \tilde{\mathbf{e}}_i \mathbf{E}_2; \quad \gamma_i = \tilde{\gamma}_i \mathbf{E}_3. \quad (1)$$

Audio Expression Alignment. To better preserve lip-synchronization with various audio emotions, we leverage cross-modality feature alignment to predict expression param-

eters. Specifically, we first fuse audio feature and emotion feature and compute the correlation matrix as

$$\mathbf{C}_{ve} = \mathcal{F}(\mathbf{v}, \mathbf{e}) \mathbf{W}_{q,1} \mathbf{W}_{k,1}^T \mathcal{F}(\mathbf{v}, \mathbf{e})^T, \quad (2)$$

where $\mathbf{W}_{q,1}, \mathbf{W}_{k,1} \in \mathbf{R}^{d \times d_h}$ are the projection matrices. \mathcal{F} denotes the fusion function from the neighboring frames, e.g., $\mathcal{F}(\mathbf{v}, \mathbf{e}) = \sum_{i-n}^i (\mathbf{v}_i + \mathbf{e}_i)$, and n is empirically set as 5. Next, we compute the correlation matrix of the text feature as:

$$\mathbf{C}_\gamma = \gamma_i \mathbf{W}_{q,2} \mathbf{W}_{k,2}^T \gamma_i^T, \quad (3)$$

where $\mathbf{W}_{q,2}, \mathbf{W}_{k,2} \in \mathbf{R}^{d \times d_h}$. Then, to better align audio and emotion feature, we fuse the two correlation matrices and obtain the attention formula as follows (denoted as “FusedAttn”):

$$\mathbf{h}_v = \text{FusedAttn}(\mathbf{v}, \mathbf{e}, \gamma) \quad (4)$$

$$= \text{Softmax}\left(\frac{\mathbf{C}_{ve} + \mathbf{C}_\gamma}{\sqrt{d_h}}\right) \mathbf{v} \mathbf{W}_{v,1}, \quad (5)$$

where $\mathbf{W}_{v,1} \in \mathbf{R}^{d \times d}$ and \mathbf{h}_v denotes the hidden state of the audio feature. Finally, we consider the fused emotion and text feature important enough to be fully learned, so we also pass and update them between separately as follows:

$$\mathbf{h}_e = \text{Softmax}\left(\frac{\mathbf{C}_{ve}}{\sqrt{d_h}}\right) \mathcal{F}(\mathbf{v}, \mathbf{e}) \mathbf{W}_{v,2} \quad (6)$$

$$\mathbf{h}_\gamma = \text{Softmax}\left(\frac{\mathbf{C}_\gamma}{\sqrt{d_h}}\right) \gamma \mathbf{W}_{v,3}, \quad (7)$$

where $\mathbf{W}_{v,2}, \mathbf{W}_{v,3} \in \mathbf{R}^{d \times d}$ and \mathbf{h}_e and \mathbf{h}_γ denote the hidden states of the emotion and the text features, respectively. At last, we have the concatenated feature $[\mathbf{h}_v; \mathbf{h}_e; \mathbf{h}_\gamma]$, which is sent to feed-forward networks to predict expression parameter $\tilde{\alpha}$. Note that $\tilde{\alpha}$ is supervised by the α from 3DMM expression coefficients [12].

B. Expression Refinement

There remains a non-trivial challenge that the predicted $\tilde{\alpha}$ can not precisely generate target emotion. The rendered frame with “happy” emotion displays expression collapse of twinkling eyebrows in the bottom-right of Fig. 2. A simple method is to pre-set certain dimension of expression parameter $\tilde{\alpha}$ to edit the emotion, for example setting $\dim_6 = -2.1$ (depicted in Fig.1 of Appendix.A) to alleviate coupled emotion representation, but not all dimensions of expression parameters are relevant to specific emotion individually.

To this end, we employ emotion specific hyperplanes to explore the entangled expression parameter space, depicted in the bottom right part of Fig. 2. These hyperplanes, pre-trained by frames of emotion specified talking head videos, enable the model to determine the boundary of emotion concept and refine parameter $\tilde{\alpha}$ to ***semantic expression parameters***. Specifically, the hyperplane is set as classifier in the expression parameter space \mathcal{A} . We define $\{y^+, y^-\}$ to label the target emotion parameters \mathcal{A}^+ and parameters for other emotions \mathcal{A}^- . The hyperplane parameter is defined as $\mathbf{w}_z \in \mathbf{R}^m$ with respect to emotion z . After obtaining the trained hyperplanes (see Appendix.B for training details), the frames can be

generated and refined via predicted expression parameter along the normal vector direction:

$$\tilde{\alpha} = \text{FFN}_1([\mathbf{h}_v; \mathbf{h}_e; \mathbf{h}_\gamma]), \tau = \text{FFN}_2([\mathbf{h}_v; \mathbf{h}_e; \mathbf{h}_\gamma]) \quad (8)$$

$$\hat{\alpha} = \tilde{\alpha} + \tau \mathbf{w}_z^T \quad (9)$$

$$\hat{\mathbf{I}} = g(\hat{\alpha}), \quad (10)$$

where FFN refers to feed-forward network, τ determines a learnable weight of manipulation, $\tilde{\alpha} \in \mathcal{A}$ refers to the predicted expression parameter and g is the expression rendering module to generate frame $\hat{\mathbf{I}}$ and will be introduced in next section. Therefore, the emotion consistency of rendered talking head is enhanced by changing the expression parameter along the direction of normal vector, resulting in “happy” emotion with relaxed eyebrows in bottom right part of Fig. 2.

C. Expression Rendering Module

Neural Radiance Fields for EmoHead. Different from previous audio-driven reconstruction methods [2], [25], we present an expression-conditioned neural radiance field. We apply implicit function with inputs of a viewing direction \mathbf{d} , a 3D location \mathbf{x} , and refined expression parameters $\hat{\alpha}$. This implicit function θ is realized by multi-layer perceptron (MLP). By combining the input vectors $(\hat{\alpha}, \mathbf{d}, \mathbf{x})$, the MLP estimates colors \mathbf{c} and densities σ of rays. This implicit function is formulated as $\theta : (\hat{\alpha}, \mathbf{d}, \mathbf{x}) \rightarrow (\mathbf{c}, \sigma)$. Similar to the rendering process in NeRF [7], the expected color \mathcal{C} of a camera ray $\mathbf{r}(t) = \mathbf{o} + t\mathbf{d}$, with a camera center \mathbf{o} , viewing direction \mathbf{d} , is integrated from near bound t_n and far bound t_f :

$$\mathcal{C}(\mathbf{r}; \theta, \mathcal{W}, \hat{\alpha}) = \int_{t_n}^{t_f} \sigma_\theta(\mathbf{r}(t)) \cdot \mathbf{c}_\theta(\mathbf{r}(t), \mathbf{d}) \cdot T(t) dt \quad (11)$$

$$T(t) = \exp\left(\int_{t_n}^t \sigma_\theta(\mathbf{r}(s)) ds\right). \quad (12)$$

Along the rays casted through each pixel, emotional talking head is computed by volume rendering process which accumulates the sampled density σ_θ and RGB values \mathbf{c}_θ , predicted by the implicit function θ . $\mathcal{W} = \{R, \omega\}$ is the predicted rigid pose parameters of the face, containing a rotation matrix $R \in \mathbf{R}^{3 \times 3}$ and a translation vector $\omega \in \mathbf{R}^{3 \times 1}$.

To obtain final synthesized output, we leverage face parsing [26] for separating torso part of talking person and background image. Note that we focus on facial emotion so that we does not discuss the performance of torso part synthesis. The final outcome frame is the concatenation of rendered head part, segmented torso part and arbitrary background.

D. Training

Many-to-one Audio-expression Module. We aim to train a universal audio-expression module that can estimate expression parameters α from arbitrary voice input. To this end, we leverage contrastive learning that audio features from different individuals are assigned to emotional parameters for same z :

$$\mathcal{L}_{reg}^{const} = \|\alpha_v^A - \hat{\alpha}_v^A\|_2 + \rho \|\alpha_v^{\bar{A}} - \hat{\alpha}_v^{\bar{A}}\|_2 \quad (13)$$

$$\hat{\alpha} = \tilde{\alpha} + \tau \mathbf{w}_z^T, \quad (14)$$

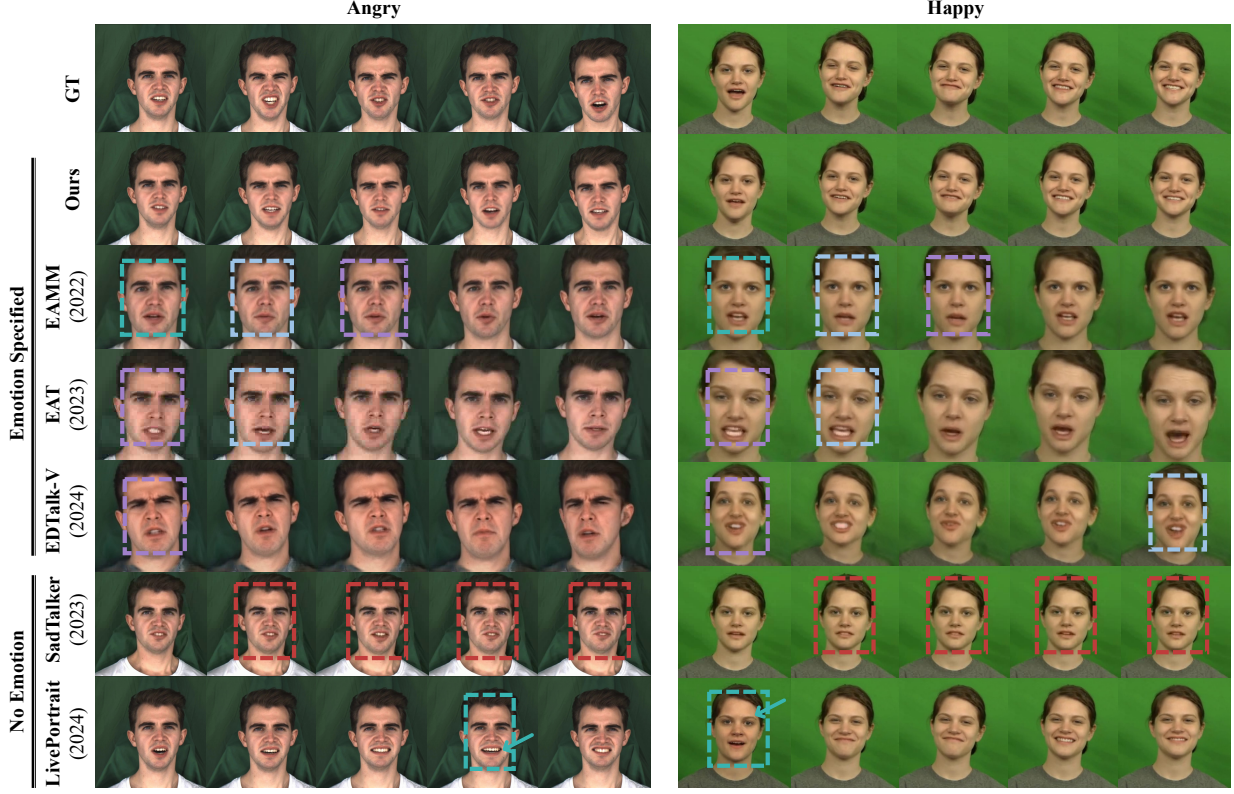


Fig. 3: Visualization comparisons of generated frames with state-of-the-art methods. See the illustration of color in Sec.IV-C.

where $\hat{\alpha}_v^A$ refers to the post-refined expression parameters given audio feature from individual A , ρ is the hyperparameter that control the degree for learning universal facial expression parameters, empirically set as 0.5. \mathbf{w}_z^T is the trained hyperplane that separate expression parameters of emotion tag z from the rest emotion tags for expression refinement. During training stage, α_v^A is randomly sampled from training set that belongs to another individual. Thus the audio-expression module is able to estimate emotion parameters from different individual for same emotion tag z .

Reconstruction Loss. We provide 2-stage reconstruction loss \mathcal{L} to train implicit function coarsely and finely:

$$\mathcal{L} = \mathcal{L}_{photo} + \mathcal{L}_{refine}. \quad (15)$$

Specifically, during first half of training stage, let $\mathbf{I}_r = \sum_{\mathbf{r}} \mathcal{C}(\mathbf{r})$ be the rendered image and \mathbf{I}_g be the groundtruth image, we minimize the photo-metric error by $\mathcal{L}_{photo} = \|\mathbf{I}_r - \mathbf{I}_g\|_2$ that coarsely reconstructs target person. Next, we utilize geometry parameters $\beta_{id} \in \mathbb{R}^{50}$ [12] to ensure implicit function for better representation of specific individual. Besides, since different person may show different expression for same emotion tag, we use CLIP [16] loss to guide the generated frame to be semantically consistent with required emotion. In detail, given the emotion tag text emo , we have:

$$\mathcal{L}_{refine} = \underbrace{-E_I(\mathbf{I}_r)^T E_T(emo)}_{\mathcal{L}_{cord}} + \underbrace{\|\beta_{id} - \hat{\beta}_{id}\|_2}_{\mathcal{L}_{shape}}, \quad (16)$$

where E_I and E_T refer to image encoder and text encoder in CLIP, respectively. We adopt \mathcal{L}_{refine} in the second-half of training stage, using \mathcal{L}_{cord} for target emotion text-image coordination, and \mathcal{L}_{shape} for enhancing reconstruction quality of target person. Finally, the weight set $\{\lambda_{photo}, \lambda_{cord}, \lambda_{shape}\}$ is applied to achieve training stability.

IV. EXPERIMENTS

A. Experiment Setup

Dataset. We apply the multi-view emotional audio-visual dataset (MEAD) [27] and the crowd-sourced emotional multimodal actors dataset (CREMA-D) [28]. MEAD contains 60 expressive actors and actresses who express eight distinct emotions at three varying intensity levels. CREMA-D [28] consists of 7,442 original clips from 91 actors, each with four different emotion levels. **Baseline Methods.** We compare EmoHead against non-emotional methods and emotion-specific methods. For non-emotional methods, we choose SadTalker [17] and LivePortrait [15]. We use the original test video as the driving source and the first frame as the input emotion condition. For emotion-specific methods, we preset one target emotion and compare the state-of-the-art methods EAMM [19], EDTalk [13], and EAT [10]. We implement all the default hyperparameters for the baseline methods.

Metrics. For the generated video, we use PSNR and SSIM to quantify reconstruction quality. We also evaluate the generated frames using the FID [29], which measures image quality and

TABLE I: Quantitative comparison and human evaluation on MEAD dataset.

Methods	SSIM \uparrow	PSNR \uparrow	M/F-LMD \downarrow	FID \downarrow	AUE \downarrow	Sync. \uparrow	ER \uparrow	Fidelity \uparrow	Coherence \uparrow	Empathy \uparrow
SadTalker [17]	0.606	19.042	2.038/2.335	69.2	2.86	5.68	52.11	3.2	3.8	3.2
LivePortrait [15]	0.720	26.161	1.314/1.572	59.5	2.05	6.96	61.82	3.3	3.5	2.9
EAMM [19]	0.610	18.867	2.525/2.814	31.3	2.35	1.76	31.08	2.7	2.9	3.5
EAT [10]	0.652	20.007	1.750/1.668	34.6	1.48	7.98	64.40	2.7	3.8	4.0
EDTalk-V [13]	0.769	22.771	1.102/1.060	38.5	1.56	6.89	68.85	2.8	3.1	3.7
Ours	0.891	28.262	1.031/0.981	30.9	1.41	8.08	73.28	4.6	4.3	4.2
Groundtruth	-	-	-	-	-	7.36	79.65	4.9	4.7	4.4

TABLE II: Quantitative comparison and human evaluation on CREMA-D dataset.

Methods	SSIM \uparrow	PSNR \uparrow	M/F-LMD \downarrow	FID \downarrow	AUE \downarrow	Sync. \uparrow	ER \uparrow	Fidelity \uparrow	Coherence \uparrow	Empathy \uparrow
SadTalker [17]	0.688	25.572	2.851/2.156	63.7	2.01	5.99	69.59	3.4	3.7	3.8
LivePortrait [15]	0.873	28.985	1.411/1.503	33.6	1.94	6.02	70.13	3.5	3.6	3.6
EAMM [19]	0.650	21.910	2.751/2.824	35.6	2.19	3.22	40.72	3.2	3.1	3.3
EAT [10]	0.794	23.712	1.925/1.791	32.3	1.98	5.70	61.76	3.1	3.7	3.5
EDTalk-V [13]	0.753	27.641	1.228/1.137	40.5	1.81	5.57	54.46	3.0	2.9	3.2
Ours	0.914	31.621	1.191/1.035	29.3	1.55	6.11	75.98	4.5	4.7	4.3
Groundtruth	-	-	-	-	-	7.09	82.51	4.9	4.8	4.8

diversity. Additionally, we employ the action unit error (AUE) [30] and face landmark distances (F-LMD) for evaluating the accuracy of face motion; the SyncNet score (Sync.) [31] and mouth landmark distances (M-LMD) [32] for assessing lip synchronization; and the accuracy of emotion recognition (ER) [33] in frames to evaluate the emotion consistency of generated video with target emotion.

B. Quantitative Analysis

Comparison with Baseline Methods. Tab. I and II shows the reconstruction quality produced by our proposed framework. Our method achieves the highest SSIM and PSNR scores, resulting in high-quality talking head videos. The AU error and F-LMD from proposed method consistently show the highest results on both datasets, illustrating that our approach also generates more realistic face motion and accurate expression than emotion-aware method EAMM, EDTalk-V and EAT. It indicates that the proposed audio-expression module successfully enhances the correlation between facial movement and audio input. As for the accuracy comparison of facial expression generation, we calculate mean accuracy of across all the emotions in the test set. We surpass the state-of-the-art method EDTalk which generates accurate target emotion of talking head. This is due to the emotion-specific hyperplane disentangles expression parameters at low-dimension space and regularize NeRF to increase the semantic representation of emotional talking head synthesis.

Ablation Studies. Please kindly refer to Appendix (D&F) for the audio expression alignment, expression refinement and loss implementation.

Human Evaluation. We conduct generation quality and emotion-based pairwise preference test for EmoHead. For a given pair of generated video and emotion tag, we assign crowd sourcing workers to annotate the video with a score on scale of 0 to 5 and report average scores. We define three aspects for evaluation: Fidelity, Coherence, and Empathy.

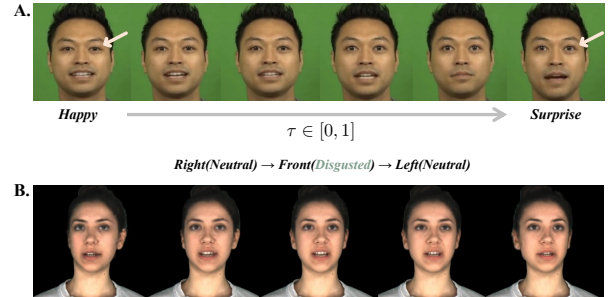


Fig. 4: (A) Continuous expression manipulation in talking stage. (B) Reconstruction result of unseen views and varying emotion. Please refer to the supplementary video.

Fidelity refers to the reconstruction quality of generated video. Coherence assesses the consistency of emotion with expression. Empathy refers to the degree to which each video encourages the user to respond with emotion. Tab. I and II show that the generated talking heads from our model exhibit higher fidelity and coherence, indicating that refined expression parameters lead to more accurate emotion representation. Our model also outperforms all the baselines in terms of empathy, evoking user for a more emotional experience.

C. Qualitative Analysis

Comparison with Baseline Methods. We provide visual examples of specific emotions to demonstrate the efficacy of the proposed method. Emotional talking heads are generated using input audio clips corresponding to each respective emotion for all methods. In Fig. 3, our method shows the best fidelity for talking head synthesis compared to the other methods. We use different colors to highlight the shortcomings of the baselines: (1) Generated output from SadTalker is limited to the source image, resulting in an output sequence that lacks of expression variability. (2) LivePortrait generates inappropriate emotions

since the mouth region displays unexpected shapes and angles that do not semantically correspond to anger. (3) EAMM, EAT, and EDTalk-V are unable to generate the same identity as the target person. (4) EAMM, EAT, and EDTalk-V fail to generate high-fidelity talking faces. Our method successfully generates consistent facial emotion without showing expression collapse.

Refinement Efficacy. Please kindly refer to Appendix (B&E) for the efficacy of the proposed methods in Sec.III-A & III-B.

Continuous Expression As shown in Fig. 4.A, our method can produce continuous facial expression changes by Eq. (10) that linearly interpolates between two expression parameters from different emotion tags during the talking stage, which cannot be accomplished by the baselines. Additionally, based on the neural radiance field, our method can generate talking head videos from unseen views with expression variation, which facilitates continuous talking head syntheses of different views and emotions, as depicted in Fig. 4.B. Please refer to the supplementary video.

V. CONCLUSION

In this paper, we present emotional talking head generation using emotion tag and refined expression parameter from a morphable face model. We provide a novel framework that includes an audio-express module for predicting expression parameters from audio input and an expression rendering module for generating person-specific talking head videos. The predicted facial expression parameters can be manipulated using pre-trained hyperplanes for expression refinement. Experimental results show that the proposed framework is effective for emotion-controllable talking head synthesis.

Acknowledgments. This work is supported in part by NSFC Project (62176061) and Shanghai Municipal Science and Technology Major Project (No.2021SHZDZX0103).

REFERENCES

- [1] KR Prajwal, Rudrabha Mukhopadhyay, Vinay P Namboodiri, and CV Jawahar, “A lip sync expert is all you need for speech to lip generation in the wild,” in *ACM MM*, 2020.
- [2] Yudong Guo, Keyu Chen, Sen Liang, Yong-Jin Liu, Hujun Bao, and Juyong Zhang, “Ad-nerf: Audio driven neural radiance fields for talking head synthesis,” in *ICCV*, 2021, pp. 5784–5794.
- [3] Linsen Song, Wayne Wu, Chen Qian, Ran He, and Chen Change Loy, “Everybody’s talkin’: Let me talk as you want,” *IEEE Transactions on Information Forensics and Security*, vol. 17, pp. 585–598, 2022.
- [4] Yaosen Chen, Yu Yao, Zhiqiang Li, Wei Wang, Yanru Zhang, Han Yang, and Xuming Wen, “Hyperlips: Hyper control lips with high resolution decoder for talking face generation,” in *arxiv*, 2023.
- [5] Shuai Tan, Bin Ji, and Ye Pan, “Style2talker: High-resolution talking head generation with emotion style and art style,” *AAAI*, 2024.
- [6] Ian Goodfellow, Jean Pouget-Abadie, Mehdi Mirza, Bing Xu, David Warde-Farley, Sherjil Ozair, Aaron Courville, and Yoshua Bengio, “Generative adversarial nets,” in *NIPS*, 2014, pp. 2672–2680.
- [7] Ben Mildenhall, Pratul P. Srinivasan, Matthew Tancik, Jonathan T. Barron, Ravi Ramamoorthi, and Ren Ng, “Nerf: Representing scenes as neural radiance fields for view synthesis,” in *ECCV*, 2020.
- [8] Suzhen Wang, Lincheng Li, Yu Ding, and Xin Yu, “One-shot talking face generation from single-speaker audio-visual correlation learning,” in *AAAI*, 2022.
- [9] Borong Liang, Yan Pan, Zhizhi Guo, Hang Zhou, Zhibin Hong, Xiaoguang Han, Junyu Han, Jingtuo Liu, Errui Ding, and Jingdong Wang, “Expressive talking head generation with granular audio-visual control,” in *CVPR*, 2022, pp. 3387–3396.
- [10] Yuan Gan, Zongxin Yang, Xihang Yue, Lingyun Sun, and Yi Yang, “Efficient emotional adaptation for audio-driven talking-head generation,” in *ICCV*, October 2023, pp. 22634–22645.
- [11] Volker Blanz and Thomas Vetter, “A morphable model for the synthesis of 3d faces,” in *SIGGRAPH*, 1999.
- [12] Jianzhu Guo, Xiangyu Zhu, Yang Yang, Fan Yang, Zhen Lei, and Stan Z Li, “Towards fast, accurate and stable 3d dense face alignment,” in *ECCV*, 2020.
- [13] Shuai Tan, Bin Ji, Mengxiao Bi, and Ye Pan, “Edtalk: Efficient disentanglement for emotional talking head synthesis,” in *ECCV*. Springer, 2025, pp. 398–416.
- [14] Yifeng Ma, Suzhen Wang, Zhipeng Hu, Changjie Fan, Tangjie Lv, Yu Ding, Zhidong Deng, and Xin Yu, “Styletalk: One-shot talking head generation with controllable speaking styles,” *arXiv preprint arXiv:2301.01081*, 2023.
- [15] Jianzhu Guo, Dingyun Zhang, Xiaoqiang Liu, Zhizhou Zhong, Yuan Zhang, Pengfei Wan, and Di Zhang, “Liveportrait: Efficient portrait animation with stitching and retargeting control,” *arXiv preprint arXiv:2407.03168*, 2024.
- [16] Alec Radford; et al., “Learning transferable visual models from natural language supervision,” in *ICML*, 2021.
- [17] Wenzuan Zhang, Xiaodong Cun, Xuan Wang, Yong Zhang, Xi Shen, Yu Guo, Ying Shan, and Fei Wang, “Sadtalker: Learning realistic 3d motion coefficients for stylized audio-driven single image talking face animation,” *CVPR*, 2023.
- [18] Sefik Emre Eskimez, You Zhang, and Zhiyao Duan, “Speech driven talking face generation from a single image and an emotion condition,” *arXiv preprint arXiv:2008.03592*, 2020.
- [19] Xinya Ji, Hang Zhou, Kaisiyuan Wang, Qianyi Wu, Wayne Wu, Feng Xu, and Xun Cao, “Eamm: One-shot emotional talking face via audio-based emotion-aware motion model,” in *ACM SIGGRAPH*, 2022.
- [20] Shuai Tan, Bin Ji, Mengxiao Bi, and Ye Pan, “Edtalk: Efficient disentanglement for emotional talking head synthesis,” *ECCV*, 2024.
- [21] Benjamin van Niekerk, Marc-André Carboneau, Julian Zaïdi, Matthew Baas, Hugo Seuté, and Herman Kamper, “A comparison of discrete and soft speech units for improved voice conversion,” in *ICASSP*, 2022.
- [22] Ziyang Ma, Zhiheng Zheng, Jiaxin Ye, Jinchao Li, Zhiyu Gao, Shiliang Zhang, and Xie Chen, “emotion2vec: Self-supervised pre-training for speech emotion representation,” *arXiv preprint arXiv:2312.15185*, 2023.
- [23] Zhifu Gao, Zerui Li, Jiaming Wang, Haoneng Luo, Xian Shi, Mengzhe Chen, Yabin Li, Lingyun Zuo, Zhihao Du, Zhangyu Xiao, and Shiliang Zhang, “Funasr: A fundamental end-to-end speech recognition toolkit,” in *INTERSPEECH*, 2023.
- [24] Hugo Touvron; et al., “Llama: Open and efficient foundation language models,” *arXiv:2302.13971*, 2023.
- [25] Zhenhui Ye, Tianyun Zhong, Yi Ren, Jiaqi Yang, Weichuang Li, Jiawei Huang, Ziyue Jiang, Jinzheng He, Rongjie Huang, Jinglin Liu, et al., “Real3d-portrait: One-shot realistic 3d talking portrait synthesis,” in *ICLR*, 2024.
- [26] Changqian Yu, Changxin Gao, Jingbo Wang, Gang Yu, Chunhua Shen, and Nong Sang, “Bisenet v2: Bilateral network with guided aggregation for real-time semantic segmentation,” *IJCV*, vol. 129, no. 11, pp. 3051–3068, 2021.
- [27] Kaisiyuan Wang, Qianyi Wu, Linsen Song, Zuoqian Yang, Wayne Wu, Chen Qian, Ran He, Yu Qiao, and Chen Change Loy, “Mead: A large-scale audio-visual dataset for emotional talking-face generation,” in *ECCV*, 2020.
- [28] Houwei Cao, David G. Cooper, Michael K. Keutmann, Ruben C. Gur, Ani Nenkova, and Ragini Verma, “Crema-d: Crowd-sourced emotional multimodal actors dataset,” *IEEE Transactions on Affective Computing*, vol. 5, no. 4, pp. 377–390, 2014.
- [29] Martin Heusel, Hubert Ramsauer, Thomas Unterthiner, Bernhard Nessler, and Sepp Hochreiter, “Gans trained by a two time-scale update rule converge to a local nash equilibrium,” in *NIPS*, 2017.
- [30] Tadas Baltrusaitis, Amir Zadeh, Yao Chong Lim, and Louis-Philippe Morency, “Openface 2.0: Facial behavior analysis toolkit,” in *International Conference on Automatic Face and Gesture Recognition*, 2018.
- [31] J. S. Chung and A. Zisserman, “Out of time: automated lip sync in the wild,” in *Workshop on Multi-view Lip-reading, ACCV*, 2016.
- [32] Lele Chen, Ross K Maddox, Zhiyao Duan, and Chenliang Xu, “Hierarchical cross-modal talking face generation with dynamic pixel-wise loss,” in *CVPR*, 2019.
- [33] Debin Meng, Xiaojiang Peng, Kai Wang, and Yu Qiao, “Frame attention networks for facial expression recognition in videos,” in *ICIP*, 2019.

- [34] Xinya Ji, Hang Zhou, Kaisiyuan Wang, Wayne Wu, Chen Change Loy, Xun Cao, and Feng Xu, “Audio-driven emotional video portraits,” in *CVPR*, 2021, pp. 14080–14089.
- [35] Pascal Paysan, Reinhard Knothe, Brian Amberg, Sami Romdhani, and Thomas Vetter, “A 3d face model for pose and illumination invariant face recognition,” in *2009 Sixth IEEE International Conference on Advanced Video and Signal Based Surveillance*, 2009, pp. 296–301.
- [36] R. Li, K. Bladin, Y. Zhao, C. Chinara, O. Ingraham, P. Xiang, X. Ren, P. Prasad, B. Kishore, J. Xing, and H. Li, “Learning formation of physically-based face attributes,” in *CVPR*, Los Alamitos, CA, USA, jun 2020, pp. 3407–3416, IEEE Computer Society.
- [37] Linchao Bao, Xiangkai Lin, Yajing Chen, Haoxian Zhang, Sheng Wang, Xuefei Zhe, Di Kang, Haozhi Huang, Xinwei Jiang, Jue Wang, Dong Yu, and Zhengyou Zhang, “High-fidelity 3d digital human head creation from rgb-d selfies,” *ACM Trans. Graph.*, vol. 41, no. 1, nov 2021.
- [38] Xiyi Chen, Marko Mihajlovic, Shaofei Wang, Sergey Prokudin, and Siyu Tang, “Morphable diffusion: 3d-consistent diffusion for single-image avatar creation,” *IEEE Conference on Computer Vision and Pattern Recognition (CVPR)*, 2024.
- [39] Haotian Yang, Hao Zhu, Yanru Wang, Mingkai Huang, Qiu Shen, Ruigang Yang, and Xun Cao, “Facescape: A large-scale high quality 3d face dataset and detailed riggable 3d face prediction,” in *CVPR*, June 2020.
- [40] Lizhen Wang, Zhiyua Chen, Tao Yu, Chenguang Ma, Liang Li, and Yebin Liu, “Faceverse: a fine-grained and detail-controllable 3d face morphable model from a hybrid dataset,” in *CVPR*, June 2022.
- [41] Shunyu Yao, RuiZhe Zhong, Yichao Yan, Guangtao Zhai, and Xiaokang Yang, “Dfa-nerf: Personalized talking head generation via disentangled face attributes neural rendering,” *arXiv preprint arXiv:2201.00791*, 2022.
- [42] Fabian Pedregosa, Gaël Varoquaux, Alexandre Gramfort, Vincent Michel, Bertrand Thirion, Olivier Grisel, Mathieu Blondel, Peter Prettenhofer, Ron Weiss, Vincent Dubourg, et al., “Scikit-learn: Machine learning in python,” *Journal of machine learning research*, vol. 12, no. Oct, pp. 2825–2830, 2011.
- [43] Shuhan Wang, Bin Shen, Xu Min, Yong He, Xiaolu Zhang, Liang Zhang, Jun Zhou, and Linjian Mo, “Aligned side information fusion method for sequential recommendation,” in *Companion Proceedings of the ACM Web Conference 2024*, New York, NY, USA, 2024, WWW ’24, pp. 112–120, Association for Computing Machinery.
- [44] Jiaxiang Tang, Kaisiyuan Wang, Hang Zhou, Xiaokang Chen, Dongliang He, Tianshu Hu, Jingtuo Liu, Gang Zeng, and Jingdong Wang, “Real-time neural radiance talking portrait synthesis via audio-spatial decomposition,” *arXiv preprint arXiv:2211.12368*, 2022.
- [45] Alec Radford, Jong Wook Kim, Chris Hallacy, Aditya Ramesh, Gabriel Goh, Sandhini Agarwal, Girish Sastry, Amanda Askell, Pamela Mishkin, Jack Clark, Gretchen Krueger, and Ilya Sutskever, “Learning transferable visual models from natural language supervision,” in *ICML*. 2021, vol. 139 of *Proceedings of Machine Learning Research*, pp. 8748–8763, PMLR.
- [46] Ashish Vaswani, Noam Shazeer, Niki Parmar, Jakob Uszkoreit, Llion Jones, Aidan N Gomez, Łukasz Kaiser, and Illia Polosukhin, “Attention is all you need,” in *NIPS*, 2017.

APPENDIX OF EMOHEAD

A. Entangled Expression Parameters in 3DMM

The 3D Face Morphable Model (3DMM) has been a fundamental area of natural face reconstruction, first proposed by Blanz et al. [11] in 1999. Initially developed as a linear model using the PCA algorithm, 3DMM is capable of representing the shape and texture of a 3D face model. Subsequent research has focused on enhancing its performance through the utilization of larger 3D face datasets [35]–[37].

Recent 3D face datasets exhibit improved diversity in expression parameters. [38] demonstrates superior generalization in facial expression fitting and other datasets [39], [40] with rich facial expressions has been collected to enhance the incorporation of facial expression bases into 3DMM. The extracted facial expression parameters from a 2D avatar satisfies continuous facial expression change through a given range. Recently, due to the continuous expression change, depicted in Figure 5.B, previous work [10], [25], [41] leverage the estimated expression parameters to represent emotion in talking head video.

However, facial expression parameters do not semantically represent target emotion. Take the reconstruction result from 3DDFA [12] as example, In Figure 5.A, by changing the value of a single dimension, we find that only a few dimensions can display interpretable facial expressions with respect to target emotion. For instance, the “angry” emotion is shown only by the eye region after setting Dim.6 = 2.1, as indicated by the red box in Figure 5.A. Nevertheless, most dimensions do not represent specific emotions, as shown by the green boxes. For example, after changing “Dimension 6” from Dim.6 = 2.1 to Dim.6 = -2.1, the “angry” emotion is lessened but shifted into an unclear emotion. Those unclear emotions lead to “**expression collapse**” phenomenon and potentially decrease generation quality of emotional talking head. In this work, we aim to disentangle the facial expression parameters to ensure specific emotion of talking head, which is crucial for generating high-quality and emotionally natural talking head video.

B. Emotion Hyperplane

Pre-training hyperplane. In this section, we introduce the training details for the hyperplane designed to distinguish facial expressions corresponding to desired emotions from other emotions. Firstly, we employ 3DDFA [12] to transform video frames of the target character in the training dataset into facial expression parameters. After the transformation into facial parameters, we label all the parameters based on their emotional tags. Subsequently, using these emotional labels, we train a hyperplane using SVM in Scikit-learn [42]. To ensure that the expression parameters effectively adapt to varying mouth openings during speech, we utilize facial landmarks to categorize five arithmetic groups, defined by the maximum and minimum of the MAR (mouth aspect ratio). During training, we evenly sample and balance the quantities across these five groups. After obtaining the trained hyperplanes, we apply them

to adjust the expression parameters to the target emotion, as depicted in the lower-left part of Figure 2 (in the main paper). **The efficacy of the emotion hyperplane.** In Table III, we compare our method with baseline emotional talking head synthesis in terms of emotion manipulation. To the best of our knowledge, we are the first to combine emotion variations in talking, which benefits emotional human-machine interaction. Here we conclude the efficacy and novelty of our proposed method:

(1) Through this emotion refinement method, we can successfully manipulate expressions based on their normal vectors for talking heads. For instance, if we aim to make an expression appear happier, we can move along the normal vector of happiness and apply a weighted coefficient in the opposite direction. We provide all six emotion variations in the CREMA-D dataset, as depicted in Figure 6. Additionally, Figure 7 demonstrates that the edited emotions are more semantically accurate than those of the baselines (EVP [34] and EDTalk [13]), particularly in the mouth regions. Consequently, through this plug-and-play method, we enhance the representation of the facial parameters obtained after prediction from audio input to expression parameters. Please refer to the emotion variations within two emotions and views in the supplementary video (approximately at the 3:45 mark).

(2) The emotion hyperplane improves the reconstruction quality of representing specific emotions. Figure 8 illustrates two refined emotions of the same character. Our proposed expression refinement method, along with the emotion hyperplane, semantically enhances generation quality and alleviate “expression collapse” phenomenon, as shown in the gray boxes of Figure 8. Surprisingly, the character’s eyes appear smaller in our method for the emotion “Contempt”, which performs even better than the ground truth.

(3) The proposed hyperplane is beneficial for generating talking heads of two different emotions in talking stage, which can not be accomplished by previous work. Specifically, we adopt the trained hyperplanes from two different emotions, denoted as w_1 and w_2 . During the inference stage, we substitute w_1 with w_2 in the pre-determined time and linearly probe them with the weight τ . We demonstrate that the generated face can successfully represent the combined emotion with the semantic expression in a single video clip. Please refer to the emotion variations during the talking stage in the supplementary video, which is located in the application section (approximately at the 4:45 mark).

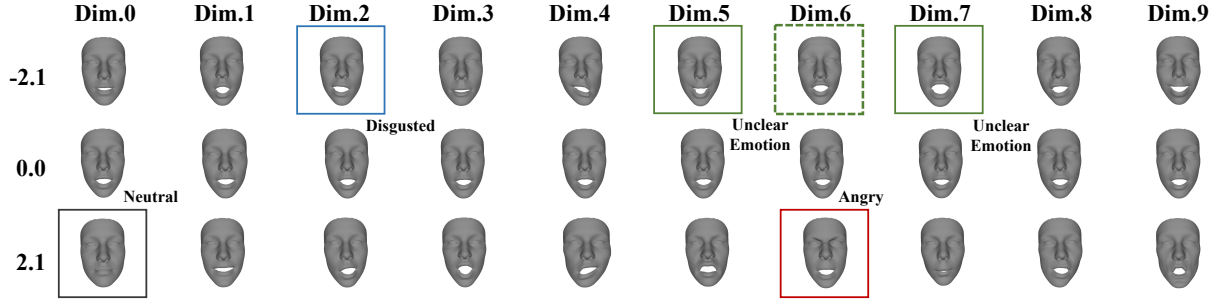
C. Implementation and Training Details

Implementation Details. First, in the Audio-Expression module, we are inspired by the Fused Attention module of [43] but Emohead has different domains and series window of model input. The input data consists of audio o and the frames per second (FPS) is set to 25 to synchronize the audio input with the video frames. Concurrently, we employ FunASR [23] to transcribe audio to text. This transcription is timestamped, allowing us to correlate the audio with its corresponding timestamps. For instance, at the i -th frame, we

TABLE III: Comparison with Baselines in terms of emotion manipulation. “-” denotes that the method is not able to achieve the function. “3DMM Exp.” refers to the expression coefficients in 3DMM [12]

Method	Manipulation Source	Varying Within Two Emotions	Varying Views	Varying Different Emotions In Talking
LivePortrait, 2024 [15]	-	-	-	-
SadTalker, 2023 [17]	Emotion Encoding (audio)	✓	-	-
EVP, 2020 [34]	-	-	-	-
EAMM, 2022 [19]	-	-	-	-
EAT, 2023 [10]	CLIP (text)	-	-	-
EDTalk, 2024 [13]	Emotion Encoding (audio & text)	✓	✓	-
Ours	3DMM Exp. (hyperplane)	✓	✓	✓

A. Expression Parameters



B. Continuous Expression Change

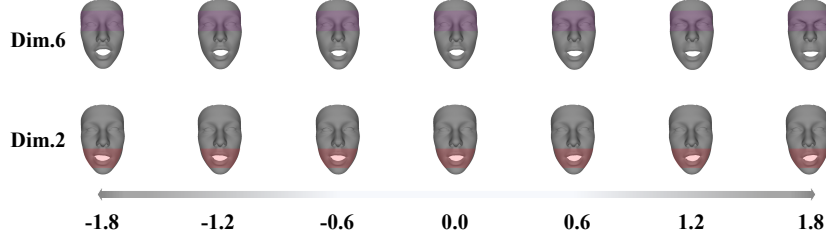


Fig. 5: Figure A displays the monocular reconstruction by changing the value of each dimension for the expression parameters of 3DMM. Emotions can hardly be reconstructed using facial expression parameters. Most dimensions represent “unclear” emotions, as depicted in the green boxes. Figure B shows the continuous expression change in a single dimension through the range $[-1.8, 1.8]$.

obtain an audio segment o_i and the corresponding text segment \mathbf{u}_j . Furthermore, within the fusion function of \mathcal{F} , the length n of neighboring frame frames is set to 5. Since the initial audio segments have an insufficient number of neighboring frames, we employ silence segment padding to fill the gaps, as illustrated in Figure 9.

Then, we provide Table V to display the detailed feature dimensions in our framework. Note that the dimension of the hyperplane \mathbf{w} corresponds to the expression coefficients of 3DMM [12], where $\alpha \in \mathbb{R}^{10}$. For the two feedforward networks in the audio expression module (Sec.III.A of the main paper), we use the same network architecture $(512, 256, 256, 128, k)$, where $k = 10$ for predicting expression parameters α and $k = 1$ for predicting hyperplane weights τ .

For the rendering module, we choose the instant-npg version of AD-NeRF [44] to achieve better efficiency of training

and inference. The implicit function θ has the same network architecture in [7].

Training Details of Two datasets. For both datasets, we use PyTorch and NVIDIA A100 to conduct all the experiments. To train the audio-expression module, all the parameters are updated with Adam optimizer with initial learning rate 0.0005. We train audio-expression module for 20k iterations and rendering module for 200k iterations. We apply \mathcal{L}_{refine} after 100k iterations. To train the implicit function in rendering module, we set 200,000 iterations for both datasets. In the first 100,000 iterations (first-half stage), we implement reconstruction loss with the Adam optimizer and a linear learning schedule. Then, we employ \mathcal{L}_{cord} and \mathcal{L}_{shape} at the second-half training stage. Within \mathcal{L}_{cord} , the CLIP image encoder E_I is CLIP-RN50 and text encoder E_T is the network fine-tuned on GPT-2 [45]. The weights of loss are set to $\lambda_{photo} = 1$, $\lambda_{cord} = 1e-3$ and $\lambda_{shape} = 1e-9$, correspondingly, to

ensure a steady and effective training process.

Differently, for the MEAD dataset, we crop the training videos to dimensions of 512×512 , with each individual providing 10 minutes of training data and 2 minutes of testing data. For the CREMA-D dataset, which is smaller than MEAD, the training videos are cropped to 340×340 , with 2 minutes of video for training data and 1 minute of video for testing data.

D. Ablation Studies of Quantitative Analysis

We quantitatively evaluate the effectiveness of audio expression alignment and expression refinement:

- w/o audio expression alignment: We use simple feature fusion method, that is, we sent the concatenated feature $[v; e; \gamma]$ to a typical self-attention transformer [46] for predicting expression parameter and hyperplane weights.
- w/o hyperplane refinement: We does not implement expression refinement $\hat{\alpha} = \tilde{\alpha} + \tau w_z^T$ for rendering talking head. Instead, the input of rendering module is $\hat{\alpha} = [z; \tilde{\alpha}]$, where $z \in \mathbb{N}^+$ is a integer that represent different emotion tags.

As shown in the top part of Table IV, the reconstruction quality without audio expression alignment decreases significantly, showing much lower SSIM and PSNR scores. Furthermore, it indicates that by enhancing the correlation between audio features and emotional features, we can better align audio features with the transcript, leading to improved lip synchronization and showing higher Sync and M-LMD score. Regarding expression refinement, we observe that without this refinement, the performance of emotion representation decreases, as indicated by lower AUE and ER score. This suggests that expression refinement enhances the emotion representation for talking head synthesis.

In order to explore how the coefficients of the 3D Face Morphable Model affect our method, we compare the expression parameters of three prevalent models. We choose MorphableDiffusion [38], FaceVerse [40], and 3DDFA [12] to regress the expression parameters for the audio-expression module. We implement dimensions of 100, 50, and 10 for the expression parameters of MorphableDiffusion, FaceVerse, and 3DDFA, respectively. Table IV demonstrates the similar performance of the three sets of expression parameters. This indicates that we can leverage 3DDFA as the source expression parameter model due to its higher runtime efficiency without compromising the quality of reconstruction.

In the third part of Table IV, we compare the size of the hidden dimension for audio expression alignment, denoted as d . It can be observed that using dimension of 512 significantly achieves better performance than 256, but there are no significant improvements when the dimension exceeds 512. Thus, for computation efficiency, we directly set $d = 512$.

In the bottom part of Table IV, we provide a comparison of the number of neighboring frames n for different fused functions in audio expression alignment. The $n = 5$ configuration outperforms the others, except in the case of ER when $n = 12$.

However, the lip synchronization for $n = 12$ is significantly lower than for $n = 5$, so we use $n = 5$ in our experiments.

E. Efficacy of Audio Expression Alignment

Based on the proposed audio expression module, our method can generate emotional talking head videos with different emotion tags, regardless of the emotion conveyed in the audio input. Figure 11 demonstrates that we generate three distinct emotions in different individuals using an audio input with “fear” emotion. Our proposed audio expression alignment successfully maps various emotional audio inputs to the desired emotional expressions, regardless of audio emotion and gender identification. Please refer to the supplementary video for detailed generation comparison (approximately at the 2:21 mark).

F. Loss Implementation

We provide Figure 10 to visualize the reconstruction results of different loss implementations. On both datasets, we observe that \mathcal{L}_{cord} improves the expression in the eye region, showing a brighter and more energetic expression in the green box. \mathcal{L}_{shape} further enhances the generation quality by displaying more accurate lip motion. By combining \mathcal{L}_{cord} and \mathcal{L}_{shape} , the results show less vagueness in the regions of the lips and teeth.

We then report quantitative ablation studies of loss implementation in Table VI. We adopt the root mean squared error (RMSE) for the expression parameters from the audio-expression module. The contrastive loss $\mathcal{L}_{reg}^{const}$ enhances the audio-expression module by alleviating the deterioration caused by person-specific audio features. The CLIP loss \mathcal{L}_{cord} improves expression recognition accuracy, making the faces closer to the target emotion. Lastly, adding identification shapes with \mathcal{L}_{shape} results in a lower AUE, indicating more vivid facial motion.

We also report the hyperparameters of the loss functions, specifically the ρ in the contrastive loss $\mathcal{L}_{reg}^{const}$ and weight set $\{\lambda_{photo}, \lambda_{cord}, \lambda_{shape}\}$ for the reconstruction loss \mathcal{L} . In the third part of Table VI, $\rho = 0.5$ performs the best, while $\rho = 1$ is the worst across the two datasets. This indicates that when the weight of other individual components increases, it decreases the performance of expression parameter prediction. In the bottom part of Table VI, we can observe by up-weighting the \mathcal{L}_{cord} , the ER value is increasing, the ER value increases, which is consistent with the findings of the \mathcal{L}_{cord} ablation study in second part of Table VI. However, When increasing the $\{\lambda_{cord}, \lambda_{shape}\}$ at, the same time, the reconstruction quality and emotion representation both decrease. We eclectically apply $\{\lambda_{photo}, \lambda_{cord}, \lambda_{shape}\} = \{1, 1e - 3, 1e - 9\}$ for our experiments, as it provides the top two performances.

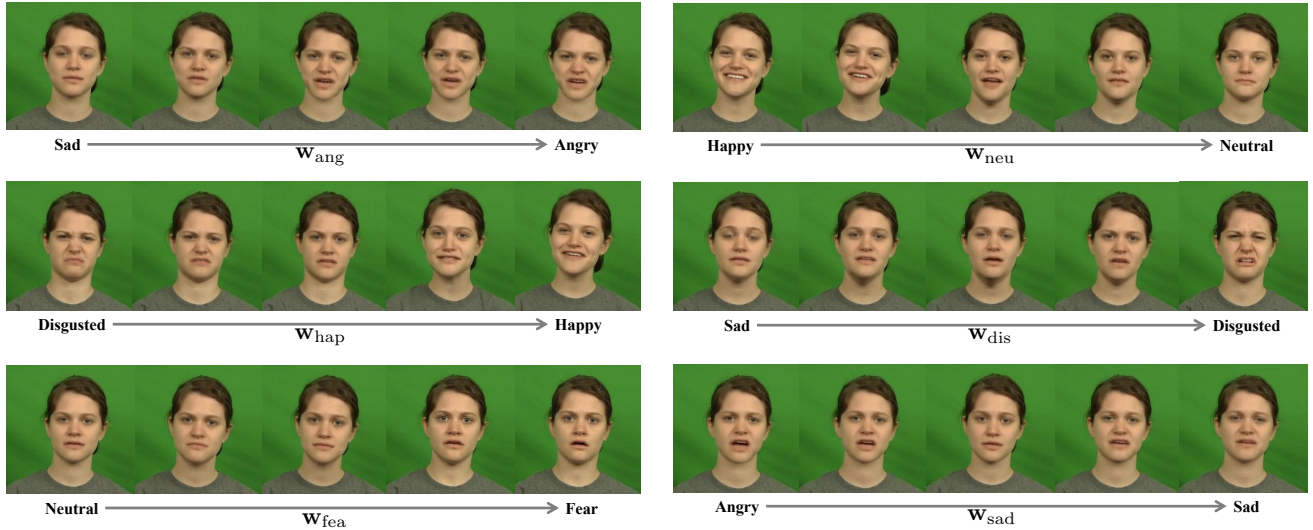


Fig. 6: Talking-stage visualization of probing expression parameters through trained hyperplane for all six emotions in CREMA-D dataset.

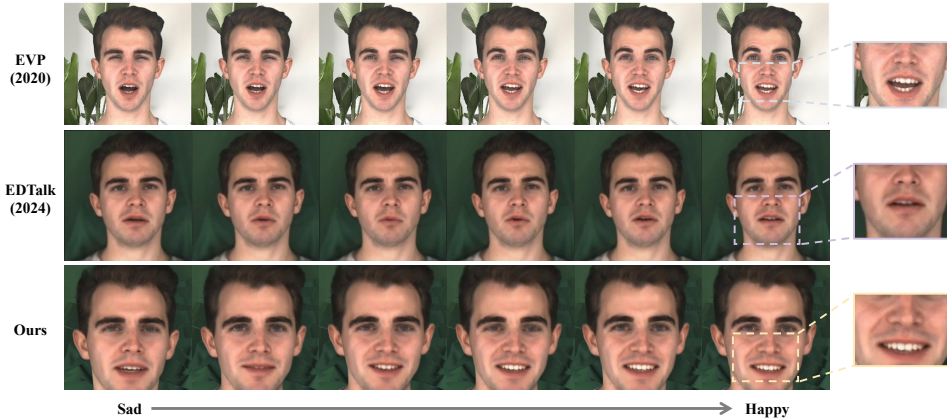


Fig. 7: Comparison of expression editing between two emotions. We enlarge the mouth region for better visualization.

TABLE IV: Quantitative comparison of ablation studies on MEAD dataset.

Settings	SSIM \uparrow	PSNR \uparrow	M/F-LMD \downarrow	FID \downarrow	AUE \downarrow	Sync. \uparrow	ER \uparrow
w/o audio expression alignment	0.730	25.191	1.149/1.082	89.6	1.95	6.19	63.44
w/o hyperplane refinement	0.872	27.410	1.291/1.203	59.2	1.86	7.25	61.29
Ours	0.891	28.262	1.031/0.981	30.9	1.41	8.08	73.28
Ours (FaceVerse) [40]	0.872	27.740	1.175/1.225	43.3	1.52	7.39	61.88
Ours (MorphableDiffusion) [38]	0.886	27.731	1.130/1.066	38.1	1.55	7.01	70.31
Ours (3DDFA) [12]	0.891	28.262	1.031/0.981	30.9	1.41	8.08	73.28
$d, d_h = 256, 256$	0.717	27.018	1.092/1.119	33.7	1.66	6.58	66.26
$d, d_h = 512, 512$	0.891	28.262	1.031/0.981	30.9	1.41	8.08	73.28
$d, d_h = 768, 768$	0.872	28.155	1.087/1.121	31.3	1.36	7.05	72.57
$d, d_h = 1024, 1024$	0.852	27.719	1.093/1.139	33.5	1.44	7.96	70.61
$n = 3$	0.803	26.114	1.072/1.087	34.6	1.56	6.77	69.31
$n = 5$	0.891	28.262	1.031/0.981	30.9	1.41	8.08	73.28
$n = 8$	0.869	27.256	1.064/0.991	31.6	1.49	7.58	72.17
$n = 12$	0.885	28.223	1.105/1.076	32.9	1.45	7.96	74.42

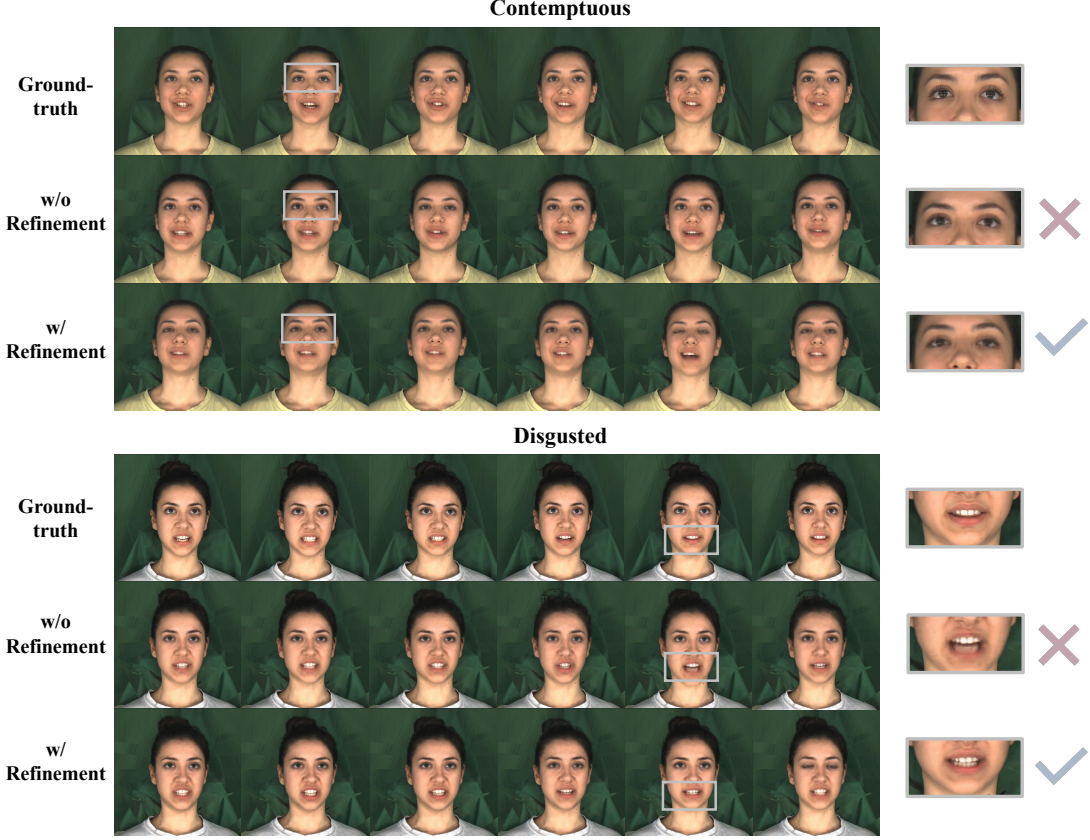


Fig. 8: Additional results of expression refinement. Gray boxes display the refined region of expression.

TABLE V: Details of Feature Dimensions.

Description	Encoder	Size
Dimension of Audio feature \tilde{v}	HuBERT-base	768
Dimension of Audio Emotion Feature \tilde{e}	Emotion2vec-base	768
Dimension of Text feature $\tilde{\gamma}$	LLaMA2-7B	4096
The Hidden Dimension for Audio Expression Alignment and projection matrix d, d_h	-	512, 512
Dimension of Emotion Hyperplane m	-	10

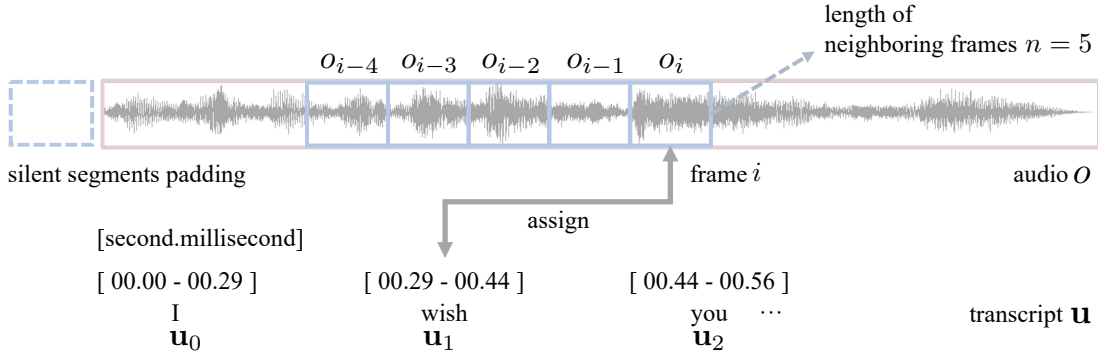


Fig. 9: Implementation details for aligned audio and transcript inputs. We assign the word u_j to audio o_i based on timestamp.

TABLE VI: Ablation Studies of loss implementation. We display the best outcome in bold and second-best in underline.

\mathcal{L}_{reg}	$\mathcal{L}_{reg}^{const}$	\mathcal{L}_{cord}	\mathcal{L}_{shape}	MEAD				CREMA-D			
				RMSE \downarrow	M/F-LMD \downarrow	AUE \downarrow	ER \uparrow	RMSE \downarrow	M/F-LMD \downarrow	AUE \downarrow	ER \uparrow
✓				0.45	-	-	-	0.39	-	-	-
✓	✓			0.27	-	-	-	0.16	-	-	-
✓	✓	✓		-	1.176/1.099	1.52	66.53	-	1.233/1.179	1.79	69.80
✓	✓		✓	-	1.104/1.051	1.73	63.71	-	1.208/1.095	1.58	61.23
✓	✓	✓	✓	-	1.031/0.981	1.41	73.28	-	1.191/1.035	1.55	75.98
$\rho = 0.2$				0.35	-	-	-	0.22	-	-	-
$\rho = 0.5$				0.27	-	-	-	0.16	-	-	-
$\rho = 0.7$				<u>0.29</u>	-	-	-	0.25	-	-	-
$\rho = 1$				0.31	-	-	-	0.27	-	-	-
$\{\lambda_{photo}, \lambda_{cord}, \lambda_{shape}\} = \{1, 1e-2, 1e-9\}$				-	1.158/1.094	1.56	74.33	-	1.271/1.096	1.61	75.01
$\{\lambda_{photo}, \lambda_{cord}, \lambda_{shape}\} = \{1, 1e-3, 1e-8\}$				-	1.004/0.853	1.43	72.11	-	1.215/1.050	1.56	71.45
$\{\lambda_{photo}, \lambda_{cord}, \lambda_{shape}\} = \{1, 5e-3, 5e-9\}$				-	1.085/1.098	1.49	72.48	-	1.155/1.007	1.70	73.69
$\{\lambda_{photo}, \lambda_{cord}, \lambda_{shape}\} = \{1, 1e-2, 1e-8\}$				-	1.091/1.072	1.55	69.79	-	1.187/1.066	1.73	70.92
$\{\lambda_{photo}, \lambda_{cord}, \lambda_{shape}\} = \{1, 1e-3, 1e-9\}$				-	<u>1.034/0.981</u>	1.41	73.28	-	<u>1.191/1.035</u>	1.55	75.98

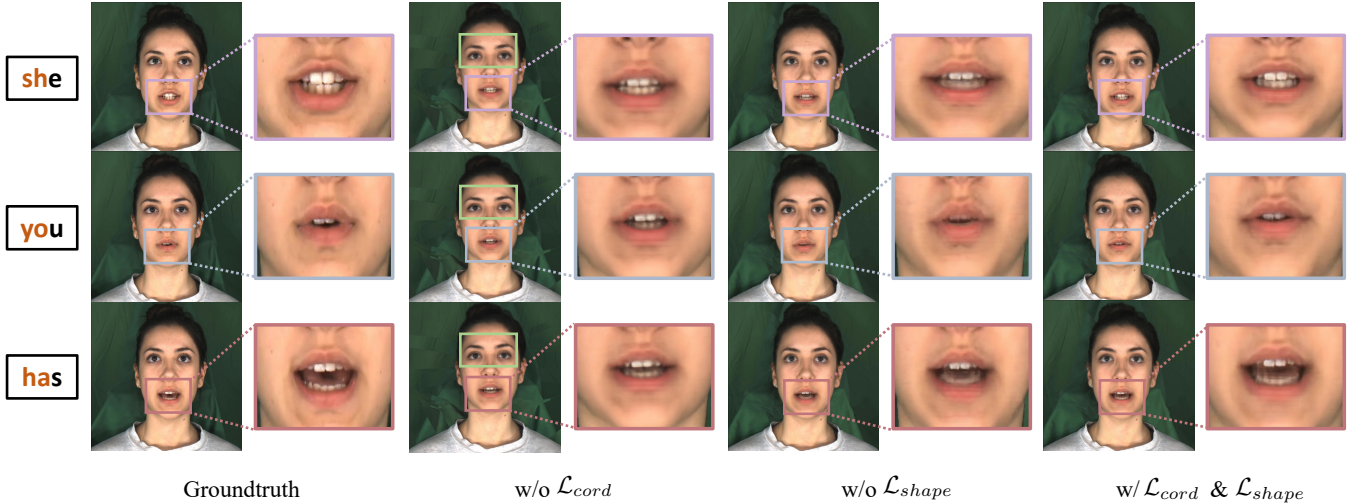


Fig. 10: Visualization of loss implementation. We present three pronunciations to compare the lips motion synthesis quality of emotional talking head.

Input audio: I am scared and I am shaking with fright.

Audio Emotion: Fear

Emotion Tag: Happy

Emotion Tag: Sad

Emotion Tag: Angry

scared



scared



fright



fright



Fig. 11: Generated results of emotional talking head with different audio emotion. We present emotion tag of **happy**, **sad**, and **angry** given audio input of **fear**.